FLY-EAR INSPIRED MINIATURE DIRECTIONAL MICROPHONES:

MODELING AND EXPERIMENTAL STUDY

H.J. Liu
Department of Mechanical Engineering
University of Maryland, College Park, USA
liuhj@umd.edu

M. Yu
Department of Mechanical Engineering
University of Maryland, College Park, USA
mmyu@umd.edu

L. Currano
U.S Army Research Laboratory
2800 Powder Mill Road, Adelphi, MD 21046, USA
LCurrano@arl.army.mil

D. Gee
U.S Army Research Laboratory
2800 Powder Mill Road, Adelphi, MD 21046, USA
danny.gee@arl.army.mil

ABSTRACT

To address the challenges in developing miniature directional microphones, a novel micro-fabricated directional microphone inspired by the superacute ears of the parasitoid fly *Ormia ocharacea* is presented in this paper. It consists of two clamped circular silicon diaphragms structurally coupled by an oxide/nitride composite bridge. The separation between the diaphragm centers is 1.25 mm, about the same size as the fly ear. A finite element model is developed to achieve a better understanding of the microphone device and guide the optimal design of the miniature microphones. Using a low coherence fiber optic interferometer detection system, the experiment shows that the directional sensitivity of this device is equivalent to a conventional microphone pair that is 9 times larger. Validating the feasibility to replicate the fly ear in a man-made structure, this work is expected to significantly impact many different fronts that require miniature sensors for sound source localization.

1. INTRODUCTION

Microphone arrays have been widely used in many applications, such as speech enhancement, sound localization, hearing aids, and noise and acoustic echo reduction [1]. Since their debut, one of the major problems that microphone arrays have been facing is the size constraint: a large size is always favorable by the point view of uniform broadband beamforming [1]. However, microphone arrays with smaller size are desirable in many aspects, for example, when there is confined space to mount devices on a micro air vehicle (MAV) or to be cosmetically acceptable for hearing impaired people. Also, not violating the far field assumption commonly used in microphone array analysis and applications, miniature microphone arrays can more effectively deal with the near-field effects [2].

However, the development of miniature microphone arrays is challenging due to the size constraint imposed by the fundamental physical law. The working of beamforming mostly relies on the estimation of the time delay of arrival (TDOA) at the microphone pair [3-6]. For a microphone pair separated by a distance d, the TDOA for an acoustic signal coming from azimuth θ is $d \sin\theta / c$, where c is the sound speed. Therefore, the microphones have to be placed bigger than a certain distance in order to resolve the minute time delay for miniature systems.

Similar scenarios occur in the nature world. To detect the direction of a sound source, humans are able to use the directional cues such as interaural intensity difference (IID), also known as interaural level difference (ILD),

interaural time difference (ITD), and the spectral composition difference [7]. However, the situation is quite different for small insects [7, 8]. First, they have limited capacity to conduct sophisticated signal processing due to the small number of neuron cells. Second, because the part of the body that the ears are placed is about 10-50 times smaller than the human head, the diffraction occurs only at high frequencies, generating negligible ILD. Third, the expected maximum time difference is in the range of tens of microseconds or even smaller, which is difficult for the insects to resolve. To tackle these challenges, they have to come up with innovative solutions, which could lead to bio-inspired new designs of directional microphone.

One striking example is found in the parasitoid fly *Ormia Ochracea*, which shows a remarkable ability to locate the calling sound (at ~ 5 kHz) of its host cricket even though its ears are separated by only 520 μm (the best possible ITD of 1.5 μs and IID of less than 1 dB) [9-12]. Studies show that the fly *Ormia ochracea* possesses a unique mechanical structure called the intertympanal bridge to couple the motions of the two tympanal membranes (eardrums) [13-15]. With such a mechanically coupled structure, the interaural intensity and time differences in the mechanical responses are amplified significantly with the values on the order of 13 dB and 50 μs, respectively [14]. The fly demonstrates in the phonotactic experiments that it can reliably locate the speaker playing the calling song by a resolution of 2° [10].

Inspired by the fly ear, Miles et al have presented pioneering work in developing miniature directional microphones [16-18]. In their design, a rigid plate supported on a flexible pivot rotates in response to the net moment generated by the pressure gradient on the external surface. Typical dimensions of these microphones are about 1 mm by 2 mm. The intention of this design is to implement a pressure gradient microphone that responds well to minute pressure gradient [17]. Saito et al proposed a design based on a circular bronze diaphragm with its center supported by a gimbal [19, 20]. The radius and thickness of the diaphragm are 10.8 mm and 30 μm. This system has one in-phase mode and two out-phase modes in order to localize the sound source in a two-dimensional plane.

We have previously reported a fly ear inspired directional microphone design and demonstrated a proof-of-concept prototype [21-23]. The aim is to fully incorporate the fly ear mechanism to the design – proper contributions from both translational and rotational modes. The prototype is made of circular Mylar diaphragms (3.5 mm radius and 22 μm thickness) coupled by steel beam bridge (25.4 mm × 1.9 mm × 0.1 mm of length × width × thickness). The device is integrated with a fiber optic interferometer system to detect the diaphragm responses to sound stimulus. Experiment shows that the fabricated device amplifies the interaural time difference (ITD) by 4.4 times and has a directional sensitivity of 6.5 μs / deg.

In this article, our recent effort of developing a miniature directional microphone at a size comparable to the fly ear is reported. In Section 2, the design of the fly ear inspired directional microphone will be detailed along with a finite element model to guide the design. Next, the fabrication process of the miniature device by micro-machining will be described in Section 3 followed by experiment results in Section 4. The article will conclude with a summary in Section 5.

2. DESIGN AND MODELING

The objective of fly-ear inspired directional microphone is not simply to "copy" the fly ear structure. Rather, it should be aimed to capture the essential dynamics of the fly-ear structure, i.e., both the rotational mode and translational mode should be utilized and their contribution should be in a proper relationship [23].

The designed bio-inspired directional microphone consists of two circular diaphragms coupled by a medially supported bridge, as shown in Figure 1. The two diaphragms are clamped on its boundary to the substrate. The ends of the bridge are connected to the diaphragm centers. In this way, the coupling force applied to the diaphragm will not excite the un-axisymmetric modes of the diaphragms, and the diaphragm has maximal deflection at its center. The pivot supports the coupling bridge in the middle and transmits the bending moment.
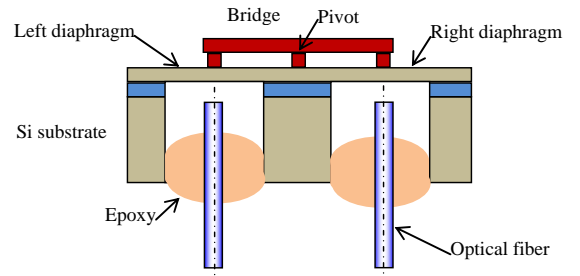

Figure 1: Design of fly ear inspired miniature directional microphone

To detect the small deflection of the diaphragms subject to a typical sound stimulus, a high-sensitivity detection method has to be adopted. Each diaphragm and the corresponding fiber tip form a Fabry-Perot cavity serving as the sensing arm in a low coherence fiber optic interferometer detection system (detailed in Section 3).

In order to design a miniature directional microphone to achieve better performance, a finite element model is created using a commercial finite element method (FEM) software ANSYS. Shell elements (SHELL63) are chosen to model both the diaphragms and the coupling bridge, as shown in Figure 2. The joints connecting the coupling

bridge and diaphragm centers are realized by using coupled DOF for intentionally placed coincident nodes (equating all translational and rotational DOFs).

To fully transmit the bending moment, ideally, the pivot is fixed but free to rotate (zero translational DOFs but free rotational DOFs), which is the case in the FEM model. If the coupling beam is otherwise fully clamped in the pivot position (zero translational and zero rotational DOFs), the left and right part of the coupling beam will be completely independent, resulting in no mechanical coupling between the two diaphragms.
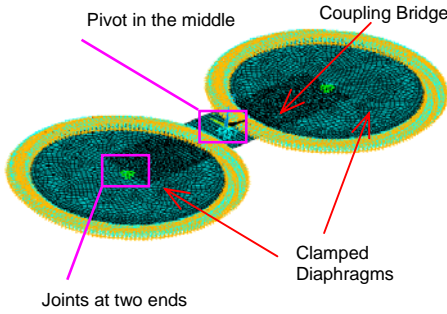

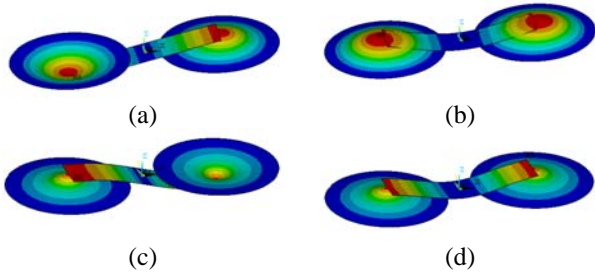Figure 2: Finite element model of the directional microphone in ANSYS

Figure 3: Vibration modes of the coupled system: (a) rocking mode for stress-free case (3.71 kHz); (b) bending mode for stress-free case (9.14 kHz); (c) rocking mode for the prestressed case ΔT=-8°C (14.65 kHz); (d) bending mode for the prestressed case ΔT=-8°C (19.69 kHz). See Table 1 for the parameters used in the FEM model.

The vibratory modes and resonances of the coupled systems can be obtained by using modal analysis. As depicted in Figure 3, the two diaphragm centers move out of phase in the rocking mode (Figure 3a) and in phase in the bending mode (Figure 3b). The mechanism of the fly ear phenomenon lies in the proper combination of these different modes. When the sound stimulus comes from the front (0° azimuth), theoretically there is no pressure difference between the two diaphragms. In this case, only the bending modes are excited, corresponding to zero mechanical interaural phase/time difference (mIPD/mITD). When the rocking mode dominates the system's response, the two diaphragms will generate close

to 180° phase difference. The relative contributions of these two modes are decided by the frequency separation, damping, the device size relative to the sound wavelength, and so on.

Table 2: Material and geometric parameters for the FEM model

Material properties of Si, SiO$_2$ and Si$_3$N$_4$				
	Young's modulus (GPa)	Poisson's ratio	Density ($\times 10^3$kg/m^3)	Thermal expansion (10^{-6}/K)
Si	140	0.27	2.3	3.0
SiO$_2$	90	0.17	2.2	0.5
Si$_3$N$_4$	290	0.24	3.1	3.3
Geometric dimensions				
Diaphragm	Poly-Si 500μm radius, and 0.5μm thickness			
Bridge	Alternating layers of SiO$_2$ and Si$_3$N$_4$; 1250μm length, 300μm width, and 3.2μm thickness (2.6μm SiO2 and 0.6μm Si3N4)			

Among the many factors that impact the characteristics of the coupled system, the inevitable thermal stress introduced in the fabrication process is one of the important issues that should be accounted for. In the FEM model, a prestressed modal analysis is carried out by applying a temperature load (ΔT) to all the nodes in the static analysis step. As illustrated in Figure 4, the coupling bridge is contracted due to negative ΔT, and pulls the diaphragm centers toward each other, generating tension in the two diaphragms. This is consistent with our previously reported observation using optical profilometer [24].

Figure 5 plots the resonance change of the rocking and bending modes as a function of the temperature change ΔT. Due to the stress-stiffening effects, the thermal stress dramatically change the two resonances. The simulation results demonstrate that it is not sufficient to design the directional microphone based on the initial-stress-free assumption. Careful characterization of thermal stress and the corresponding fabrication process is very crucial to the performance of the fabricated devices.
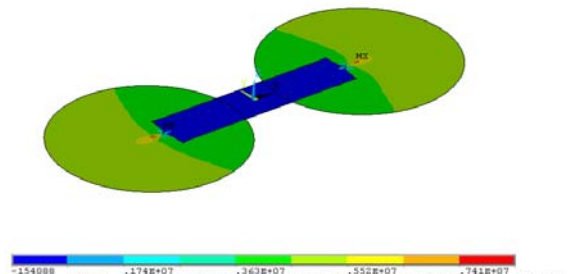

Figure 4: Thermal stress distribution (x component) when ΔT=-8°C. The x component is in radial direction for the diaphragms (local nodal coordinate system), and in axial direction for the coupling bridge.
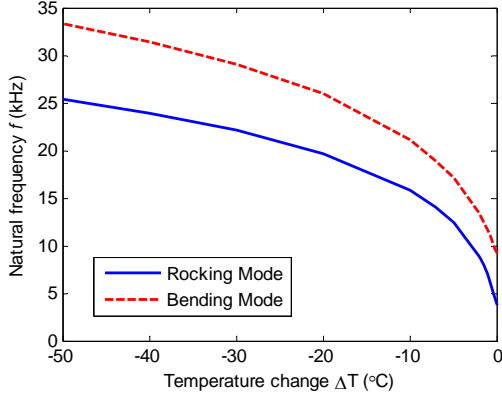
Figure 5: Effects of thermal stress on the system's natural frequencies. The thermal stress is generated by introducing a universal temperature change ΔT to the constrained system.

3. DEVICE FABRICATION

We have previously reported the fabrication process of the miniature directional microphone by micro-machining [24]. Starting from a blank double side polished silicon wafer, a 1µm thick silicon dioxide layer is deposited by plasma enhanced chemical vapor deposition (PECVD) to serve as an etch stop for the upcoming back-etching step. The SiO_2 is annealed in nitrogen at 700°C for 60s to densify the film and drive off excess trapped hydrogen. Then, a 0.5µm thick layer of polysilicon is sputtered on top of the SiO_2 as the membrane material (Figure 6a). These two deposition steps can be replaced by using a customized silicon-on-insulator (SOI) wafer. Next, a photoresist sacrificial layer is deposited and patterned on top of the polysilicon, and hard baked at 175°C. This is followed by PECVD of the coupling beam, which consists of alternating layers SiO_2 and Si_3N_4. The temperature is controlled at 175°C to avoid burning the photoresist. The final thickeness of the beam is 3.2 µm, including 2600Å SiO_2 and 600Å Si_3N_4. The coupling beam is patterned with a second layer of photoresist and etched by reactive ion etching (RIE) (Figure 6b). A photoresist layer is patterned on the backside of the wafer to define the membrane geometry. Then, the silicon wafer is etched by deep reactive ion etching (DIE) until reaching the SiO_2 etch stop layer (Figure 6c). Using the same mask, the SiO_2 layer is removed also by RIE (Figure 6d). The sacrificial photoresist is removed with an isotropic oxygen plasma ash process (Figure 6e). The final fabricated device is shown in Figure 7.
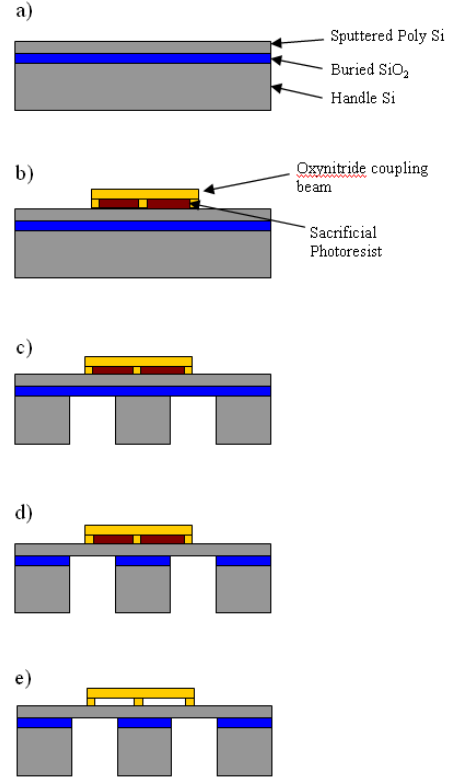

Figure 6: Microphone fabrication process [24].

To facilitate the insertion of the optical fiber to the backside of the diaphragm, a fiber guide is fabricated from a second double side polished wafer. Using an epoxy bond layer, the fiber guide chip and the microphone chip are first aligned and then bonded by heating to 200°C on a hotplate.

The final step is to insert the fiber through the guider chip and secured by using ultra-violet (UV) cured epoxy. Each diaphragm and the corresponding fiber tip forms a Fabry-Pérot (FP) interferometer, which is part of the low-coherence fiber optic interferometer (LCFOI) depicted in Figure 8. Broadband light from a super-luminescent light emitting diode (SLED) is first sent via a 3dB optical coupler CP0 to two other couplers (CP1 and CP2). At the output of each coupler, the light beam is directed to the FP sensor. The reflected light from each FP sensor is then coupled back to a tunable Fabry-Pérot filter (TF1 and TF2) and finally to a photo detector (PD1 or PD2).
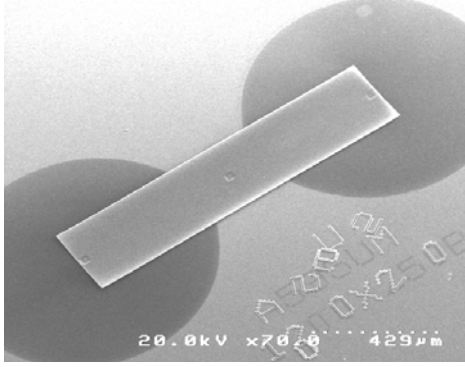
Figure 7: Coupled membrane acoustic localization microphone [24].

In the experimental setup, maximum sensitivity is achieved when initial OPD is in the vicinity of quadrature points, that is,

$$L_{si} - L_{ri} = (2m-1)\frac{1}{4}\lambda \qquad (1)$$

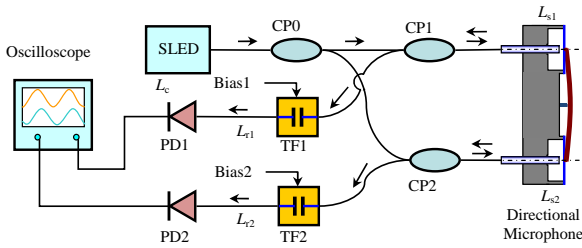where $m = 0, \pm 1, \pm 2 \cdots$.

Figure 8: A low-coherence fiber optic interferometer (LCFOI) detection system for the miniature directional microphone [23]

As opposed to the conventional FOI, LCFOI measures the differential optical phase change between a sensing interferometer and a readout interferometer. This technique can not only take advantage of the features of the conventional optical interferometer based sensors, but in addition, this technique provides much higher signal-to-noise ratio, lower drift, and more reliable sensing data, and allows for a large bandwidth, large dynamic range, and a much more simplified phase demodulation scheme [25].

4. EXPERIMENT RESULTS

To characterize the fabricated device, a band-limited white noise is first played through a speaker, and the photo-detector outputs are used to get the diaphragm response in frequency domain (FFT). A pronounced peak at 14.1 kHz can be identified corresponding to the rocking mode. This is consistent with the simulation results in Figure 3(c). However, the corresponding bending mode does not appear in the obtained spectrum, suggesting the

actual bending mode resonance might be higher than the simulation results ~20 kHz. This discrepancy can be attributed to several issues. First, the thermal process for the actual fabrication is far more complicated than the simulation scenario. Second, the working frequency of the speaker is unfortunately below 20 kHz. Actually, using the equivalent 2-DOF model [13], the bending mode is predicted to be at ~30 kHz. The bending mode resonance is expected to be captured if a speaker with wider working frequency range is used.

Figure 9 compares the phase difference mIPD of the MEMS device at 10 kHz, the 2-DOF simulation results, and the initial phase difference in the acoustic inputs. The simulation results based on the 2-DOF model is obtained by setting the rocking and bending resonances at 15 kHz and 32 kHz, and modal damping ratios at 0.01. At the midline (azimuth = 0°), the directional sensitivity of the fabricated device, defined as the change of time delay per unit azimuth change, reaches 0.54 μs/deg. This is not only great amplification of the initial acoustic input (0.063 μs/deg), but comparable to the fly ear's performance at 5 kHz (0.63 μs/deg, simulation results based on the parameters in [13]). The amplified directional sensitivity enables the devices to achieve the localization resolution of a much large conventional microphone pair. For example, when working at 10 kHz, the MEMS device is equivalent to an uncoupled microphone pair that is 9 times larger, i.e. 11.3 mm as opposed to 1.25 mm.
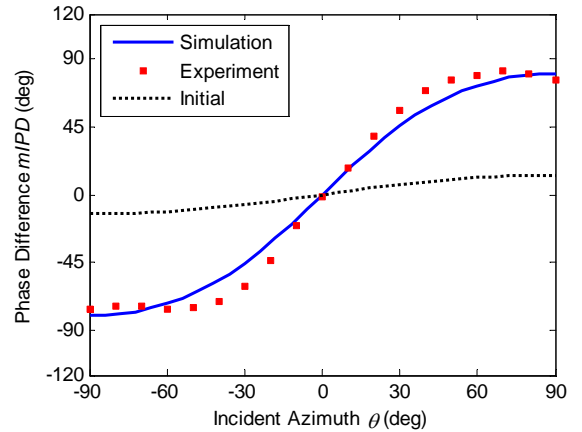

Figure 9: Phase difference as a function of incident azimuth for pure tone at 10 kHz

5. SUMMARY

The superacute ear of the parasitoid fly *Ormia ochracea* and its underlying mechanism has inspired researchers to seek novel designs to address the long-standing challenges of developing miniature directional microphones. In this article, the design of a fly ear inspired miniature directional microphone is presented. This device consists of two clamped circular diaphragms

mechanically coupled by a center-supported bridge, capturing the essential dynamics of the fly ear structure. A finite element model is developed to guide the design and fabrication of the directional microphone. As a counterpart for the previously reported proof-of-concept large scale system, the micro-machined device uses poly-silicon for the diaphragm, alternating layers of silicon oxide and silicon nitride for the coupling beam. The interaural distance (or port separation) of this device is 1.25 mm, about the same size as the separation of the centers of the fly ear tympana (eardrums). The experiment results show that the device can significantly amplify time delay in a wide frequency range (5 kHz-20kHz). When working at 10 kHz, the amplification ratio of directional sensitivity at the midline reaches 9 times, which means it is equivalent to the sensitivity obtained by a conventional microphone pair separated by 11.3 mm. Future efforts can be made to better control the fabrication process and adjust the working frequency range as per specific applications. This work lays the foundation for the development of miniature fly ear inspired directional microphone, and it can be used in many applications which require miniature sensors for sound source localization.

ACKNOWLEDGEMENTS

REFERENCES

1. Branstein, M. and D. Ward, *Microphone Arrays: Signal Processing Techniques and Applications.* 2001, New York: Springer.
2. Brooks, T.F. and W.M. Humphreys, *Effect of directional array size on the measurement of airframe noise components*, in *5th AIAA/CEAS Aeroacoustics Conference and Exhibit.* 1999: Bellevue, WA. p. AIAA-1999-1958.
3. Boujemaa, H., et al., *Joint azimuth, elevation, and time of arrival estimation of diffuse sources.* Annales Des Telecommunications-Annals of Telecommunications, 2008. **63**(7-8): p. 425-433.
4. Chen, J.D., J. Benesty, and Y.T. Huang, *Time delay estimation in room acoustic environments: An overview.* EURASIP Journal on Applied Signal Processing, 2006: p. 1-19.
5. van der Veen, A.J., M.C. Vanderveen, and A. Paulraj, *Joint angle and delay estimation using shift-invariance techniques.* Ieee Transactions on Signal Processing, 1998. **46**(2): p. 405-418.
6. Walker, W.F. and G.E. Trahey, *A fundamental limit on delay estimation using partially correlated speckle signals.* Ieee Transactions on Ultrasonics Ferroelectrics and Frequency Control, 1995. **42**(2): p. 301-308.
7. Popper, A.N. and R.R. Fay, *Sound source Localization.* 2005, New York: Springer.
8. Hoy, R.R. and A.N. Popper, *Comparative Hearing: Insects.* 1998, New York: Springer.
9. Cade, W., *Acoustically orienting parasitoids - fly phonotaxis to cricket song.* Science, 1975. **190**(4221): p. 1312-1313.
10. Mason, A.C., M.L. Oshinsky, and R.R. Hoy, *Hyperacute directional hearing in a microscale auditory system.* Nature, 2001. **410**(6829): p. 686-690.
11. Robert, D., J. Amoroso, and R.R. Hoy, *The evolutionary convergence of hearing in a parasitoid fly and its cricket host.* Science, 1992. **258**(5085): p. 1135-1137.
12. Walker, T.J., *Phonotaxis in female Ormia ocharacea (Dipetera, Tachinidae), a parasitoid of field crickets.* Journal of Insect Behavior, 1993. **6**(3): p. 389-410.
13. Miles, R.N., D. Robert, and R.R. Hoy, *Mechanically coupled ears for directional hearing in the parasitoid fly Ormia ochracea.* Journal of the Acoustical Society of America, 1995. **98**(6): p. 3059-3070.
14. Robert, D., R.N. Miles, and R.R. Hoy, *Directional hearing by mechanical coupling in the parasitoid fly Ormia ochracea.* Journal of Comparative Physiology a-Sensory Neural and Behavioral Physiology, 1996. **179**(1): p. 29-44.
15. Robert, D., R.N. Miles, and R.R. Hoy, *Tympanal mechanics in the parasitoid fly Ormia ochracea: intertympanal coupling during mechanical vibration.* Journal of Comparative Physiology a-Neuroethology Sensory Neural and Behavioral Physiology, 1998. **183**(4): p. 443-452.
16. Cui, W., et al., *Optical sensing in a directional MEMS microphone inspired by the ears of the parasitoid fly, Ormia Ochracea.* The 19th IEEE International Conference on Micro Electro Mechanical Systems 2006: p. 614-617.
17. Miles, R.N., et al., *A low-noise differential microphone inspired by the ears of the parasitoid fly Ormia ochracea.* Journal of the Acoustical Society of America, 2009. **125**(4): p. 2013-2026.
18. Yoo, K., et al., *Fabrication of biomimetic 3-D structured diaphragms.* Sensors and Actuators A - Physical, 2002. **97-8**: p. 448-456.
19. Ono, N., A. Saito, and S. Ando, *Design and experiments of bio-mimicry sound source localization sensor with gimbal-supported circular diaphragm*, in *12th International Conference on Solid State Sensors, Actuators and Microsystems.* 2003: Boston. p. 935-938.

20. Saito, A., N. Ono, and S. Ando, *Micro gimbal diaphragm for sound source localization with mimicking Ormia Ochracea*, in *41st SICE Annual Conference*. 2002. p. 2159-2162.
21. Liu, H.J., Z. Chen, and M. Yu, *Biology-inspired acoustic sensors for sound source localization*, in *SPIE Smart Materials/NDE*. 2008: San Diego, CA, USA. p. 69322Y.
22. Liu, H.J., M. Yu, and X.M. Zhang, *Biomimetic optical directional microphone with structurally coupled diaphragms.* Applied Physics Letters, 2008. **93**(24).
23. Liu, H.J., X.M. Zhang, and M. Yu, *Understanding fly-ear inspired directional microphones*, in *SPIE Smart Materials/NDE*. 2009: San Diego, CA, USA. p. 72922M.
24. Currano, L., et al., *Microscale implementation of a bio-inspired acoustic localization device*, in *SPIE Conference on Defense, Secuirity and Sensing*. 2009: Orlando, FL, USA. p. 73210B.
25. Yu, M., *Fiber-optic sensor systems for acoustic measurements*, in *Mechanical Engineering*. 2002, University of Maryland: College Park, MD.